POLITECNICO DI TORINO
Repository ISTITUZIONALE

Reduced Nodal Admittance Matrix Method for Probabilistic GIC Analysis in Power Grids

(Article begins on next page)

09 April 2024

Reduced Nodal Admittance Matrix Method for Probabilistic GIC Analysis in Power Grids

Min-zhou Liu, *Graduate Student Member, IEEE,* Yan-zhao Xie, *Senior Member, IEEE,* Yi-fan Yang,
Riccardo Trinchero, *Member, IEEE,* and Igor S. Stievano, *Senior Member, IEEE*

Abstract—**Efficient probabilistic geomagnetically induced current (GIC) analysis in power grids provides tools for assessing and mitigating small-probability tail risks of geomagnetic disturbances, especially in early warning and real-time scenarios. This letter employs the reduced nodal admittance matrix (RNAM) to speed up GIC calculation based on Kron reduction. Moreover, the proposed RNAM method is used to achieve a more efficient analysis of probabilistic GICs, which considers the uncertainty of the substation grounding resistances. The novel method is compared with the classical algorithms including the nodal admittance matrix method, the Lehtinen-Pirjola method, and the bus admittance matrix method, and its efficiency improvement is illustrated with several power grid test cases.**

Index Terms—**Geomagnetic disturbances, geomagnetically induced currents, Kron reduction, nodal admittance matrix, uncertainty quantification.**

I. INTRODUCTION

GEOMAGNETIC disturbances (GMDs) initiated by the solar activity generate geomagnetically induced currents (GICs) in the bulk transmission networks, which may lead to adverse effects such as voltage collapse and transformer hot-spot heating [1], [2]. Accurate GIC modeling is challenged by uncertain DC resistance parameters in the power grid. In this context, efficient probabilistic GIC analysis plays a key role in developing robust online operational mitigation schemes against uncertain GMD hazards, e.g. generation redispatch, GIC blocking device action and emergency control.

The efficiency improvement of power grid GIC calculation has attracted much attention in recent years. The nodal admittance matrix (NAM) method [1] and the Lehtinen-Pirjola (LP) method [2] are derived on the basis of the full-node circuit model, i.e. all the substation grounding grids and buses are regarded as nodes, which results in a large-scale system of linear equations. Recently, Marsal *et al.* [3] proposed a bus

admittance matrix (BAM) method for GIC model reduction, and the newly created matrix to be inverted is asymmetric.

This letter proposes a more efficient GIC calculation method based on Kron-reduced nodal admittance matrix (RNAM) [4], which can be easily implemented on the basis of the classical full-node NAM method. It can reduce the size of the computational model and preserve the positive definiteness of the matrix, thus it can be efficiently solved by utilizing Cholesky decomposition. Furthermore, the proposed RNAM method is applied to the probabilistic GIC analysis considering the uncertainty of substation grounding resistance parameters [5]. The calculation procedure is accelerated by the proposed RNAM method, which is demonstrated by several power grid test cases [6]–[9].

II. CLASSICAL FULL-NODE NAM METHOD

Consider a transmission network affected by GMD, including n_g substations, n_b buses and n_t transformers in the GIC flow path. The effect of the wide-area distributed horizontal geoelectric field $\mathbf{E}$ can be modeled as a voltage source in the power line:

$$V_{ik}^{s} = \int_{\mathcal{L}_{ik}} \mathbf{E} \cdot \mathrm{dl} \tag{1}$$

where $\mathcal{L}_{ik}$ is the geographic path of the power line (i, k).

Then the voltage source can be converted into the current injections at buses $\mathbf{J}_b$ with Norton equivalent system, whereas the current injections at the substation grounding grid nodes $\mathbf{J}_g$ are zero:

$$\mathbf{J}_b = \mathbf{\Gamma}\mathbf{E} \in \mathbb{R}^{n_b \times T}, \ \mathbf{J}_g = \mathbf{0} \in \mathbb{R}^{n_g \times T} \tag{2}$$

where $\mathbf{\Gamma} \in \mathbb{R}^{n_b \times 2n_z}$ is the incident matrix; $\mathbf{E} \in \mathbb{R}^{2n_z \times T}$ is the induced geoelectric field matrix, n_z is the number of geological zones, and T is the number of time instants.

In the classical GIC model for a power grid with multiple voltage levels, the substation grounding grid node set $\mathcal{N}_g$ and the bus node set $\mathcal{N}_b$ are combined into a full-node set $\mathcal{N}_g \cup \mathcal{N}_b$. Then, the full-node voltages $\mathbf{V} \in \mathbb{R}^{(n_g+n_b) \times T}$ can be calculated by the NAM method [1]:

$$\mathbf{Y}\mathbf{V} = \mathbf{J} = \begin{bmatrix} \mathbf{J}_g \\ \mathbf{J}_b \end{bmatrix} \tag{3}$$

where the nodal admittance matrix $\mathbf{Y} \in \mathbb{R}^{(n_g+n_b) \times (n_g+n_b)}$ is sparse symmetric positive definite, and its nonsingularity needs to be guaranteed by a preprocessing step, i.e. removing the isolated bus nodes.

Min-zhou Liu is with the State Key Laboratory of Electrical Insulation and Power Equipment, School of Electrical Engineering, Xi'an Jiaotong University, Xi'an 710049, China, and also with the Department of Electronics and Telecommunications, Politecnico di Torino, 10129 Turin, Italy (e-mail: liuminzhou@outlook.com).

Yan-zhao Xie and Yi-fan Yang are with the State Key Laboratory of Electrical Insulation and Power Equipment, School of Electrical Engineering, Xi'an Jiaotong University, Xi'an 710049, China (e-mail: yzxie@mail.xjtu.edu.cn; yangyf@stu.xjtu.edu.cn).

Riccardo Trinchero and Igor S. Stievano are with the Department of Electronics and Telecommunications, Politecnico di Torino, 10129 Turin, Italy (e-mail: riccardo.trinchero@polito.it; igor.stievano@polito.it).
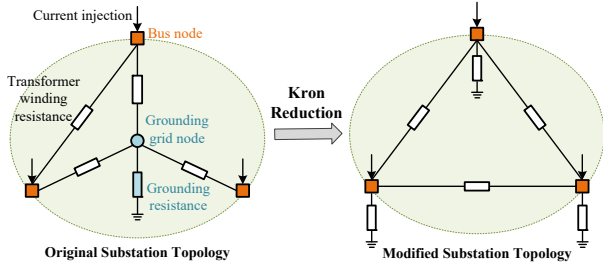
Fig. 1. Schematic diagram of substation topology modification by eliminating the substation grounding grid node based on Kron reduction.

Further, the obtained full-node voltages can be used to calculate the transformer effective GICs [1] as follows

$$\mathbf{I_t} = \mathbf{\Phi V} = \mathbf{\Phi Y}^{-1}\mathbf{J} \qquad (4)$$

where $\mathbf{\Phi} \in \mathbb{R}^{n_t \times (n_g+n_b)}$ is the transformation matrix for the transformer effective GICs.

The substation grounding GICs, depending on the voltages of the substation grounding grid nodes, can be calculated by

$$\mathbf{I_g} = \begin{bmatrix} \mathbf{Y_g} & \mathbf{0} \end{bmatrix}\mathbf{V} = \begin{bmatrix} \mathbf{Y_g} & \mathbf{0} \end{bmatrix}\mathbf{Y}^{-1}\mathbf{J} \qquad (5)$$

where $\mathbf{Y_g} = \text{diag}(R_{g,1}^{-1}, \ldots, R_{g,n_g}^{-1}) \in \mathbb{R}^{n_g \times n_g}$ is the substation grounding conductance matrix, $R_{g,i}$ is the grounding resistance of the i-th substation, and $\mathbf{0} \in \mathbb{R}^{n_g \times n_b}$ is a zero matrix.

III. PROPOSED MODEL REDUCTION FOR PROBABILISTIC GIC ANALYSIS

A. RNAM method for Nodal Voltage Calculation

In this section, we detail the model order reduction method for GIC calculation based on Kron reduction [4]. If we partition the matrices by node type, the nodal voltage equations in (3) can be rewritten as:

$$\left[\begin{array}{c|c} \mathbf{Y_{gg}} & \mathbf{Y_{gb}} \\ \hline \mathbf{Y_{bg}} & \mathbf{Y_{bb}} \end{array}\right] \cdot \left[\begin{array}{c} \mathbf{V_g} \\ \hline \mathbf{V_b} \end{array}\right] = \left[\begin{array}{c} \mathbf{0} \\ \hline \mathbf{J_b} \end{array}\right] \qquad (6)$$

It is worth noting that block $\mathbf{Y_{gg}}$ is a positive diagonal matrix since the coupling between the grounding grids of the substations through the earth can usually be ignored. Thus, its inverse $\mathbf{Y_{gg}^{-1}}$ is easy to find.

Using the voltage equations for substation grounding nodes $\mathcal{N}_g$, $\mathbf{V_g}$ can be expressed by the bus voltages $\mathbf{V_b}$ as

$$\mathbf{V_g} = -\mathbf{Y_{gg}^{-1}Y_{gb}V_b} \qquad (7)$$

Substituting (7) into the bus voltage equations in (6), the calculation of $\mathbf{V_b}$ can be reduced to

$$\widetilde{\mathbf{Y}}\mathbf{V_b} = \mathbf{J_b} \qquad (8)$$

where the reduced nodal admittance matrix $\widetilde{\mathbf{Y}} := \mathbf{Y_{bb}} - \mathbf{Y_{bg}Y_{gg}^{-1}Y_{gb}} \in \mathbb{R}^{n_b \times n_b}$ is the Schur complement of the block $\mathbf{Y_{gg}}$ of the matrix $\mathbf{Y}$ [4].

The above mathematical transformation automatically modifies the topology of each substation, i.e. eliminating the internal grounding grid node, as depicted in Fig. 1. The proposed RNAM method has the following advantages:

1) The size of the reduced matrix $\widetilde{\mathbf{Y}}$ is less than that of the full-node matrix $\mathbf{Y} \in \mathbb{R}^{(n_g+n_b) \times (n_g+n_b)}$ in (3), thus

it may reduce the storage requirements and speed up the GIC simulation without compromising the computational accuracy.
2) The matrix $\widetilde{\mathbf{Y}}$ preserves positive definiteness according to the Schur complement lemma [4].
3) The matrix $\widetilde{\mathbf{Y}}$ preserves sparsity since eliminating $\mathcal{N}_g$ does not create new non-zero entries between the buses in different substations.
4) The current injections at the bus nodes $\mathbf{J_b}$ remain unchanged.

Furthermore, the interconnected power grid may involve multiple transmission system operators. Suppose we are interested in the GMD impacts on one sub-network whose bus set is denoted as $\mathcal{N}_{b1}$. The other buses $\mathcal{N}_{b2} = \mathcal{N}_b \backslash \mathcal{N}_{b1}$ belong to the neighboring sub-networks. Then (8) can be partitioned as

$$\left[\begin{array}{c|c} \widetilde{\mathbf{Y}}_{11} & \widetilde{\mathbf{Y}}_{12} \\ \hline \widetilde{\mathbf{Y}}_{21} & \widetilde{\mathbf{Y}}_{22} \end{array}\right] \cdot \left[\begin{array}{c} \mathbf{V_{b1}} \\ \hline \mathbf{V_{b2}} \end{array}\right] = \left[\begin{array}{c} \mathbf{J_{b1}} \\ \hline \mathbf{J_{b2}} \end{array}\right] \qquad (9)$$

where the subscripts 1 and 2 in $\widetilde{\mathbf{Y}}_{ij}$, $\mathbf{V}_{bi}$ and $\mathbf{J}_{bi}(i,j = 1,2)$ correspond to the bus subsets $\mathcal{N}_{b1}$ and $\mathcal{N}_{b2}$, respectively.

Then the voltage $\mathbf{V_{b1}}$ of interest can be calculated by eliminating the bus set $\mathcal{N}_{b2}$ as follows:

$$\left(\widetilde{\mathbf{Y}}_{11} - \widetilde{\mathbf{Y}}_{12}\widetilde{\mathbf{Y}}_{22}^{-1}\widetilde{\mathbf{Y}}_{21}\right)\mathbf{V_{b1}} = \mathbf{J_{b1}} - \widetilde{\mathbf{Y}}_{12}\widetilde{\mathbf{Y}}_{22}^{-1}\mathbf{J_{b2}} \qquad (10)$$

B. RNAM-based GIC Calculation

The subsequent GIC calculation can be simplified by using the RNAM in (8). If we partition the transformation matrix by node types as $\mathbf{\Phi} = \begin{bmatrix} \mathbf{\Phi_g} & | & \mathbf{\Phi_b} \end{bmatrix}$, the formula (4) for the transformer effective GICs can be simplified as

$$\mathbf{I_t} = \mathbf{\Phi V} = \widetilde{\mathbf{\Phi}}\mathbf{V_b} = \widetilde{\mathbf{\Phi}}\widetilde{\mathbf{Y}}^{-1}\mathbf{J_b} \qquad (11)$$

where $\widetilde{\mathbf{\Phi}} := \mathbf{\Phi_b} - \mathbf{\Phi_g}\mathbf{Y_{gg}^{-1}Y_{gb}} \in \mathbb{R}^{n_t \times n_b}$ is the reduced transformation matrix.

Similarly, the formula (5) for the substation grounding GICs can be reduced to

$$\mathbf{I_g} = \mathbf{Y_g V_g} = -\mathbf{Y_g Y_{gg}^{-1}Y_{gb}V_b} = -\mathbf{Y_g Y_{gg}^{-1}Y_{gb}}\widetilde{\mathbf{Y}}^{-1}\mathbf{J_b} \qquad (12)$$

Alternatively, the substation grounding GIC can also be calculated by eliminating the bus nodes

$$\mathbf{I_g} = -\mathbf{Y_g}(\mathbf{Y_{gg}} - \mathbf{Y_{gb}Y_{bb}^{-1}Y_{bg}})^{-1}\mathbf{Y_{gb}Y_{bb}^{-1}J_b} \qquad (13)$$

where matrix $\mathbf{Y_{gg}} - \mathbf{Y_{gb}Y_{bb}^{-1}Y_{bg}} \in \mathbb{R}^{n_g \times n_g}$ is typically dense. Hence, equation (12) is more preferred than (13) for GIC calculation due to the more sparse matrix and the fewer times of inversion.

The GIC flow in the transmission lines can be useful for model validation by differential magnetometry [10]. The GIC in power line (i,k) can be calculated as:

$$I_{tl,ik} = y_{ik}\left(V_{b,i} - V_{b,k} + V_{ik}^s\right) \qquad (14)$$

where y_{ik} is the admittance of the power line (i,k), and $V_{b,i}$ and $V_{b,k}$ are the voltages of buses i and k, respectively.
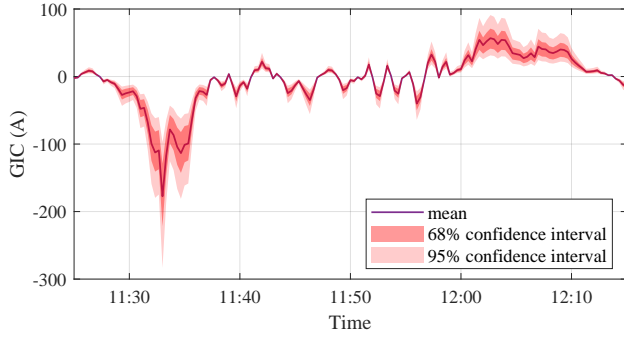
Fig. 2. Mean and confidence intervals of grounding GIC of substation 4 in EPRI-21 test case [6] during the GMD event on 2015/08/15.

C. Uncertainty Quantification of GIC

The proposed RNAM method is applied to the probabilistic GIC analysis that considers uncertain resistance parameters in the power grid. Substation grounding resistance values are a major source of GIC uncertainty, since they are usually not included in the standard power flow data and are time-varying depending on local soil conductivity [5].

The resulting uncertainty of GIC can be quantified by using the Monte Carlo method. For each sample of substation grounding resistances, we modify the substation grounding conductance matrix $\mathbf{Y}_g$ and block $\mathbf{Y}_{gg}$. The latter is further used to update the reduced admittance matrix $\widetilde{\mathbf{Y}}$ and the reduced transformation matrix $\widetilde{\mathbf{\Phi}}$. Finally we can obtain the probability distribution of the GICs with the RNAM method.

IV. Case Study

A. Probabilistic GICs in EPRI-21 Power Grid Test Case

The probabilistic GICs in the EPRI-21 test case [6] during the GMD event on 2015/08/15 are analyzed for illustration. The geomagnetic data with 1-second time cadence at Yellowknife observatory from INTERMAGNET are used as inputs. The induced geoelectric fields are then calculated by using the Québec 1D layered conductivity model [11].

The substation grounding resistances are assumed to be independently log-normally distributed. Let $\ln R_{g,i} \sim \mathcal{N}\left(\ln \bar{R}_{g,i}, (0.5 \ln \alpha)^2\right)$, where $\bar{R}_{g,i}$ is the base grounding resistance of i-th substation from [6], and α is the scaling factor. Thus, the 95% confidence interval of $R_{g,i}$ is $[\bar{R}_{g,i}/\alpha, \alpha \bar{R}_{g,i}]$. We take $\alpha = 2$ as a typical example, then the uncertainty of GIC is quantified by the Monte Carlo method. Fig. 2 depicts the grounding GIC of substation 4. The GIC magnitude at 11:33:03 is 175.6 A in the case of base resistance value, and its 95% confidence interval is [98.4, 291.1] A, which highlights the importance of uncertainty quantification for GIC.

B. Comparison of Four GIC Calculation Methods

We have compared the performance of LP, NAM, BAM and RNAM methods in calculating the substation grounding GICs. The design matrices of linear equations in the four methods are decomposed by different methods. The *LU decomposition* is used for the matrix in the LP method and the BAM method due to their asymmetry. The *Cholesky decomposition*, which is
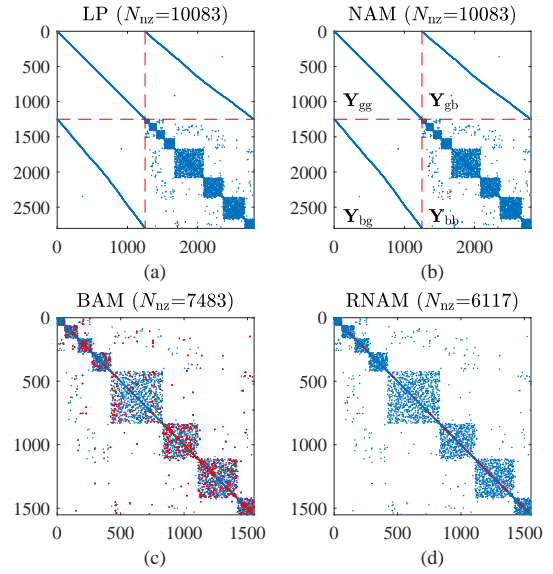

Fig. 3. Sparsity of the design matrices of the four GIC calculation methods for the ACTIVSg2000 power grid case [9]. In subfigures (a) and (b), the red dashed lines depict the boundary between the substation grounding nodes and the buses. In subfigures (c) and (d), the red scatter points show the new non-zero entries in the design matrix of the BAM and RNAM methods compared to the matrix block $\mathbf{Y}_{bb}$. In the title, N_{nz} is the number of non-zero entries in the design matrix.

more efficient than the general LU decomposition, is adopted for the matrix $\mathbf{Y}$ in the NAM method (3) and the matrix $\widetilde{\mathbf{Y}}$ in the RNAM method (8), since they are symmetric positive definite. Then the nodal voltages and GICs can be solved using the forward and backward substitution techniques.

In addition to the size and positive definiteness of the design matrix, its sparsity also affects the computational efficiency. For the ACTIVSg2000 power grid test case [9], the sparsity of the design matrices of the four methods is compared in Fig. 3. It can be seen that the design matrices of the LP and NAM methods have the same sparsity. BAM method reduces the size of the design matrix at the cost of potentially introducing a large number of new non-zero entries compared to the matrix block $\mathbf{Y}_{bb}$, whereas only few new non-zero entries are introduced in the RNAM method as shown in Fig. 3(d).

The current injections at the buses, calculated by using the geoelectric fields in subsection IV-A, are added with random components to characterize the influence of spatially nonuniform geoelectric fields. And the number of time instants is taken as $3,600 \times 24 = 86,400$ (1-second time cadence and 1-day duration).

The GIC algorithms are tested using MATLAB R2020b software on a desktop with a 4.0 GHz Intel i7-6700K CPU and 64 GB RAM. The MATLAB codes are available online [12]. The GIC results of the four methods are strictly consistent. Table I compares the total calculation time, including design matrix factorization and substation grounding GIC calculation, of the four methods for several power grid test cases. It can be seen that the RNAM method is more efficient than the classical methods. Taking the IEEE 118-GMD test case as an example, the RNAM method decreases the calculation time to 60.4%

TABLE I
COMPARISON OF ALGORITHM PERFORMANCE OF FOUR GIC CALCULATION METHODS

Test cases	Number of Monte Carlo samples	Size of design matrix*				Calculation time (s)**			
		LP	NAM	BAM	RNAM	LP	NAM	BAM	RNAM
EPRI-21 [6]	1,000	17	17	11	11	29.2	11.5	20.9	**8.5**
IEEE 118-GMD [7]	1,000	225	225	118	118	397	164	253	**99**
Sanhua UHV-EHV [8]	1,000	279	279	186	186	478	210	353	**141**
ACTIVSg2000 [9]	2,000	2,801	2,801	1,551	1,551	14,620	6,329	11,012	**4,269**

* Size n is the abbreviation for a $n \times n$ square matrix.
** MATLAB provides two built-in functions `lu` and `decomposition` for LU factorization, and two built-in functions `chol` and `decomposition` for Cholesky factorization. The calculation time here refers to the best result of different functions for sparse matrix factorization in MATLAB R2020b software. Note that the efficiency ranking of the NAM and BAM methods may change when using the full matrix factorization, which is detailed in the supplementary material [12].

of the NAM method, 24.9% of the LP method, and 39.1% of the BAM method.

V. CONCLUSION AND FUTURE WORK

This letter proposes a RNAM method for uncertainty quantification of GICs in power grids. The method makes GIC calculation more efficient than the classical full-node models, which is beneficial to time-critical online operation and control to mitigate GIC impacts. The results of several test cases show that it can save about 25%-40% of the simulation time compared with the classical full-node NAM method. Further work is in progress to evaluate the impacts of probabilistic GICs on AC voltages and transformer temperature rises by combining the method with the advanced surrogate modeling.

ACKNOWLEDGMENT

REFERENCES

[1] T. J. Overbye, K. S. Shetye, T. R. Hutchins, Q. Qiu, and J. D. Weber, "Power grid sensitivity analysis of geomagnetically induced currents," *IEEE Trans. Power Syst.*, vol. 28, no. 4, pp. 4821–4828, 2013.

[2] D. H. Boteler and R. J. Pirjola, "Comparison of methods for modelling geomagnetically induced currents," *Ann. Geophys.*, vol. 32, no. 9, pp. 1177–1187, 2014.

[3] S. Marsal, J. M. Torta, V. Canillas-Pérez, and J. J. Curto, "A new standalone tool for DC-equivalent network generation and GIC calculation in power grids with multiple voltage levels," *Space Weather*, vol. 20, no. 3, p. e2021SW002984, 2022.

[4] F. Dorfler and F. Bullo, "Kron reduction of graphs with applications to electrical networks," *IEEE Trans. Circuits Syst. I, Reg. Papers*, vol. 60, no. 1, pp. 150–163, 2013.

[5] M. Kazerooni, H. Zhu, T. J. Overbye, and D. A. Wojtczak, "Transmission system geomagnetically induced current model validation," *IEEE Trans. Power Syst.*, vol. 32, no. 3, pp. 2183–2192, 2017.

[6] R. Horton, D. Boteler, T. J. Overbye, R. Pirjola, and R. C. Dugan, "A test case for the calculation of geomagnetically induced currents," *IEEE Trans. Power Del.*, vol. 27, no. 4, pp. 2368–2373, 2012.

[7] A. Haddadi, A. Rezaei-Zare, L. Gérin-Lajoie, R. Hassani, and J. Mahseredjian, "A modified IEEE 118-bus test case for geomagnetic disturbance studies–part I: Model data," *IEEE Trans. Electromagn. Compat.*, vol. 62, no. 3, pp. 955–965, 2020.

[8] S.-X. Guo, L.-G. Liu, R. J. Pirjola, K.-R. Wang, and B. Dong, "Impact of the EHV power system on geomagnetically induced currents in the UHV power system," *IEEE Trans. Power Del.*, vol. 30, no. 5, pp. 2163–2170, 2015.

[9] A. B. Birchfield, T. Xu, K. M. Gegner, K. S. Shetye, and T. J. Overbye, "Grid structural characteristics as validation criteria for synthetic networks," *IEEE Trans. Power Syst.*, vol. 32, no. 4, pp. 3258–3265, 2017.

[10] S. Marsal, J. M. Torta, J. J. Curto, V. Canillas-Pérez, O. Cid, M. Ibañez, and A. Marcuello, "Validating GIC modeling in the Spanish power grid by differential magnetometry," *Space Weather*, vol. 19, no. 12, p. e2021SW002905, 2021.

[11] D. H. Boteler, "The evolution of Québec earth models used to model geomagnetically induced currents," *IEEE Trans. Power Del.*, vol. 30, no. 5, pp. 2171–2178, 2015.

[12] M. Liu, "RNAM-GIC," https://github.com/minzhouliu/RNAM-GIC, 2023.